Self-Decoupled MIMO Antenna Pair With Shared Radiator for 5G Smartphones

Libin Sun, *Student Member, IEEE*, Yue Li, *Senior Member, IEEE*, Zhijun Zhang, *Fellow, IEEE*, and Hanyang Wang, *Senior Member, IEEE*

***Abstract*— In this article, a novel self-decoupled multiple-input multiple-output (MIMO) antenna pair with a shared radiator is proposed for fifth-generation (5G) smartphones. In our approach, a radiator is directly excited by two feeding ports, and interestingly, the two ports are naturally isolated across a wide bandwidth without using any extra decoupling structures. To offer a deep physical insight of the self-decoupling mechanism, a mode-cancellation method based on the synthesis of common and differential modes is developed for the first time. The proposed self-decoupled antenna pair shows a good isolation of better than 11.5 dB across the 5G N77 band (3.3–4.2 GHz) with a radiation pattern diversity property. Based on the self-decoupled antenna pair, an 8 × 8 MIMO antenna system, constituted by four sets of antenna pairs, is simulated, fabricated, and measured to validate the concept. The experimental results demonstrate that the proposed 8 × 8 MIMO system can offer an isolation of better than 10.5 dB between all ports and a high total efficiency of 63.1%–85.1% across 3.3–4.2 GHz. With the advantages of self-decoupling, shared radiator, simple structure, wide bandwidth, and high efficiency, the proposed design scheme exhibits promising potential for the future highly integrated MIMO antennas for 5G smartphones.**

***Index Terms*— Antenna pair, fifth-generation (5G), mode-cancellation method (MCM), multiple-input multiple-output (MIMO), self-decoupled, smartphone antenna.**

I. Introduction

MULTIPLE-INPUT multiple-output (MIMO) is an effective technique for enhancing the channel capacity and has been considered as one of the key techniques for fifth-generation (5G) mobile communication systems [1]. The mutual coupling between MIMO antenna elements, however, will affect the orthogonality between different data streams and, thus, deteriorates the channel capacity of MIMO systems [2], [3]. To mitigate the unwanted mutual coupling, various decoupling techniques have been widely investigated in recent years [4], such as electromagnetic bandgaps [5], neutralization lines [6]–[8], parasitic decoupling elements [9], [10], decoupling network [11], *LC* tanks with resonant slots [12], strips [13] or lumped components [14], decoupling surface [15], and pattern or polarization diversity techniques [16]–[20].

In 5G mobile terminals, about eight MIMO antenna elements operating at sub-6 GHz spectrum should be accommodated in the size-limited environment and coexist with 2G/3G/4G antennas. The direct design scheme is to separate antenna elements individually and to decouple partly by the spatial distance [21]–[32]. Also, some other decoupling techniques, such as high-order mode [27], orthogonal polarizations [28], *LC* tanks [29]–[30], and self-isolated elements [31], [32], are also exploited to further improve the antenna isolation. However, the occupied footprint of MIMO antennas is overmuch in this scheme, which is not competent for practical size-limited environment.

To address the above problem and fit the size-limited environment in smartphones, two or four tightly arranged or shared-radiator MIMO antenna elements are integrated together as a building block to reduce the overall footprint with a spatial reuse [33]–[44]. In [35], neutralization line technique is employed to mitigate the mutual decoupling among four closely spaced open-slot antenna elements across 3.4–3.6 GHz to form a four-antenna building block with a compressed antenna size. In [36], two asymmetrically mirrored gap-coupled loop antennas operating at 3.4–3.6 GHz are integrated as a novel self-decoupled building block. In [37] and [38], grounded strips and distributed coupling capacitances are combined as a parallel LC tank to suppress the coupling currents between two tightly arranged loop antennas. In [39], parallel and series LC tanks are strategically united to constitute a novel tightly arranged four-antenna building block at 3.4–3.6 GHz. In [40]–[44], a novel orthogonal-mode scheme is proposed to realize a natural high isolation of more than 20 dB across 3.4–3.6 GHz between two closely spaced [40]–[42] or shared-radiator [43], [44] antenna elements without using any extra decoupling structures. The above dual-antenna or four-antenna building blocks, with high integration levels and good isolations, make great progress in the footprint reduction of MIMO antenna systems. However, the narrowband decoupling property of the above design schemes will make them encounter a bottleneck in the future global 5G New Radio (NR) business [45]. As a result, realizing wideband decoupling between tightly arranged or shared-radiator MIMO

Manuscript received August 31, 2019; revised November 8, 2019; accepted December 19, 2019. Date of publication January 8, 2020; date of current version May 5, 2020. This work was supported in part by the National Natural Science Foundation of China under Contract 61971254 and Contract 61525104, and in part by the Beijing Natural Science Foundation under Contract 4182029. *(Corresponding author: Zhijun Zhang.)*

Libin Sun, Yue Li, and Zhijun Zhang are with the Beijing National Research Center for Information Science and Technology (BNRist), Tsinghua University, Beijing 100084, China (e-mail: zjzh@tsinghua.edu.cn).

Hanyang Wang is with Huawei Technology Ltd., Reading RG2 6UF, U.K. (e-mail: hanyang.wang@huawei.com).

Color versions of one or more of the figures in this article are available online at http://ieeexplore.ieee.org.

Digital Object Identifier 10.1109/TAP.2019.2963664

0018-926X © 2020 IEEE. Personal use is permitted, but republication/redistribution requires IEEE permission.
See https://www.ieee.org/publications/rights/index.html for more information.

Authorized licensed use limited to: Tsinghua University. Downloaded on July 21,2020 at 08:32:09 UTC from IEEE Xplore. Restrictions apply.

antenna elements will become a new development trend of future 5G MIMO smartphone antennas. However, it still remains a huge challenge with few published work in the open literature [46], [47]. Wong *et al.* [46] proposed an ultrawideband (3.3–6.0 GHz) MIMO antenna pair decoupled by a center-distributed *LC* tank yet at the expense of separated element configuration. Then, a simple shared-radiator antenna pair decoupled by capacitance-based *LC* tank is also proposed with an operating band of about 3.3–4.0 GHz [47]. These two works pave the way for the wideband 5G MIMO building blocks yet at the expense of separated element configuration [46] or using extra decoupling components [47].

Here, we propose a self-decoupled MIMO antenna pair with a shared radiator to enhance the integration level of MIMO antennas and to accommodate the upcoming wideband 5G NR business. Two antenna elements are merged together as a shared-radiator antenna pair, yet a good isolation is still realized without using any extra decoupling structures. To interpret the physical mechanism of the novel self-decoupling phenomenon, a mode-cancellation method (MCM), based on the new insight of common mode (CM) and differential mode (DM) cancellation, is proposed for the first time. According to the MCM, the current mode fed through one port could be equivalent to the synthesis of the CM and DM currents. Hence, the current in half of the shared radiator is superposed, whereas that in another half is canceled out, leading to a natural self-decoupling property. To validate the concept, a planar shared-radiator antenna pair is simulated in HFSS, and the simulated isolation is better than 11.5 dB across 5G N77 band (3.3–4.2 GHz) with a good impedance matching. Based on the proposed self-decoupled antenna pair, it is readily to fulfill a self-decoupled 8 × 8 MIMO antenna system by placing four sets of antenna pairs at both side frames of the smartphone. Both the simulated and measured results demonstrate that, the 8 × 8 MIMO system shows a good isolation and diversity performance with isolations better than 10.5 dB and envelope correlation coefficients (ECCs) less than 0.2 across 3.3–4.2 GHz among all eight ports. Also, a high measured total efficiency of 63.1%–85.1% with an average value of 76.0% for all antenna elements is also achieved.

This article is organized as follows. In Section II, the MCM is addressed to interpret the operating mechanism of the self-decoupled MIMO antenna pair. In Section III, the specific design of a planar self-decoupled antenna pair is presented to validate the concept, including antenna structure, decoupling analysis, radiation performance, and diversity performance. In Section IV, an 8 × 8 MIMO system based on the proposed self-decoupled antenna pair is simulated, fabricated, and measured. Besides, a comparison table is also presented to highlight the advantages of this design scheme. In Section V, the antenna performance in practical application environments is discussed. Finally, Section VI draws a conclusion.

II. Methodology of the Self-Decoupled Antenna Pair

To clearly interpret the self-decoupling mechanism, a model of the shared-radiator antenna pair excited by two symmetric

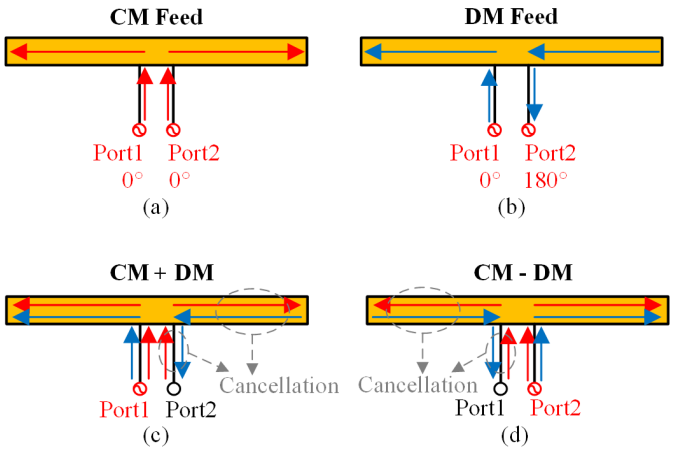

Fig. 1. Sketch diagram of a dual-port shared-radiator antenna pair and corresponding current distributions in different feeding cases. (a) CM feed. (b) DM feed. (c) In-phase synthesis of CM and DM, the current is superposed in port1 but canceled out in port2. (d) Out-of-phase synthesis of CM and DM, the current is superposed in port2 but canceled out in port1.

feeding ports is illustrated in Fig. 1. The sketch diagram of operating current modes under different feeding schemes is also depicted in Fig. 1.

When port1 and port2 are simultaneously fed with CM signals, i.e., equal amplitude and phase in two ports

$$\mathbf{I_c} = \begin{pmatrix} I_0 \\ I_0 \end{pmatrix} \tag{1}$$

an out-of-phase current mode could be excited in the shared radiator as shown in Fig. 1(a).

On the contrary, when port1 and port2 are fed simultaneously with DM signals, i.e., equal amplitude but out of phase in two ports

$$\mathbf{I_d} = \begin{pmatrix} I_0 \\ -I_0 \end{pmatrix} \tag{2}$$

A dipole-like in-phase current mode could be excited in the shared radiator as shown in Fig. 1(b).

When CM and DM signals could be generated simultaneously in the shared radiator with equal amplitude and phase, as shown in Fig. 1(c), the currents in port1 and left half of the shared radiator are enhanced, whereas those in port2 and right half of the radiator are canceled out. Therefore, port2 could be naturally isolated from port1 in this status

$$(\mathbf{I_d} + \mathbf{I_c})/2 = \begin{pmatrix} I_0 & 0 \end{pmatrix}^T. \tag{3}$$

In other words, when the shared-radiator antenna pair is fed through port1, only left half of the radiator could be effectively excited with right half of the radiator and port2 naturally isolated, which is an interesting phenomenon for the integrated MIMO antenna design.

Similarly, when CM and DM signals are superposed with equal power but out of phase, as shown in Fig. 1(d), the currents in port2 and right half of the radiator are enhanced, whereas those in port1 and left half of the radiator are canceled out. Therefore, port1 could be naturally isolated from port2 in

Authorized licensed use limited to: Tsinghua University. Downloaded on July 21,2020 at 08:32:09 UTC from IEEE Xplore. Restrictions apply.

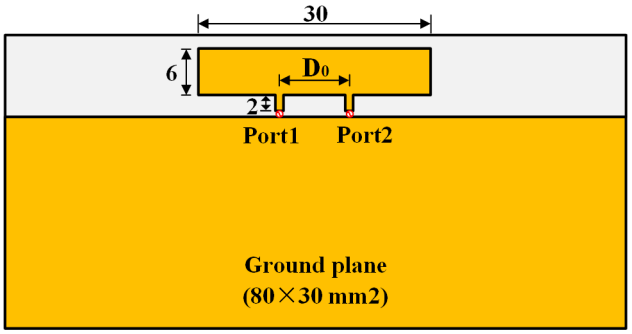

Fig. 2. Geometry of the planar self-decoupled MIMO antenna pair with a shared radiator, unit all in millimeters.

this status

$$(\mathbf{I_d} - \mathbf{I_c})/2 = \begin{pmatrix} 0 & I_0 \end{pmatrix}^T. \quad (4)$$

It should be noted that only if the CM and DM have the same active impedance, (3) and (4) can be strictly established. If the active impedance of CM is unequal with DM, the current mode superposition cannot be mapped to the feeding source superposition due to the inconsistent reflection power. Namely, the key for self-decoupling is aligning the CM and DM active impedances to a similar level, which will be discussed in detail in Section III-B from the view of scatter matrix.

III. Design of the Planar Self-Decoupled Antenna Pair

A. Antenna Structure

To verify the concept that proposed in Section II, a planar shared-radiator antenna pair is proposed and simulated in HFSS as shown in Fig. 2. The proposed antenna pair is placed above an 80 × 30 mm^2 ground plane and printed on a 0.8 mm-thick FR-4 ($\varepsilon_r = 4.4$, $\tan\delta = 0.02$) substrate. The shared rectangular radiator, with a dimension of 30 × 6 mm^2, is excited by two symmetric feeding strips individually. The two feeding ports are separated by a distance of D_0, which is a key parameter for the port isolation.

B. Decoupling Analysis

According to the theory of microwave network [48], the CM and DM active reflection coefficients can be deduced and simplified in the condition of symmetric and reciprocal 2-port network with $S_{11} = S_{22}$ and $S_{12} = S_{21}$

$$S_{cc11} = (S_{11} + S_{12} + S_{21} + S_{22})/2 = S_{11} + S_{21} \quad (5)$$

$$S_{dd11} = (S_{11} - S_{12} - S_{21} + S_{22})/2 = S_{11} - S_{21}. \quad (6)$$

Therefore, the relationship between CM and DM reflection coefficients is

$$|S_{cc11} - S_{dd11}| = 2|S_{21}|. \quad (7)$$

Equation (7) establishes a bridge between the single-ended and CM/DM 2-port networks. That is, the isolation between port1 and port2 can be equivalent to the difference between CM and DM complex reflection coefficients. The difference of complex reflection coefficients can be easily accessed by the Euclidean distance in Smith chart. Therefore, the smaller distance between CM and DM reflection coefficients, the higher isolation between port1 and port2. For example, if port1 and port2 are perfectly isolated, i.e., $S_{21} = 0$, we have $S_{cc11} = S_{dd11}$. That is to say, only CM and DM reflection coefficients are equal with each other, the out-of-phase currents in CM and DM can be canceled out absolutely with a perfect self-isolation. If port1 and port2 perform an isolation of $S_{21} < -10$ dB $= 0.316$, we have $|S_{cc11} - S_{dd11}| < 0.632$ (the radius of Smith chart is normalized to unity). Thus, we should tune the active reflection coefficients of CM and DM as similar as possible (or as closer as possible in Smith chart) for realizing a good isolation between port1 and port2.

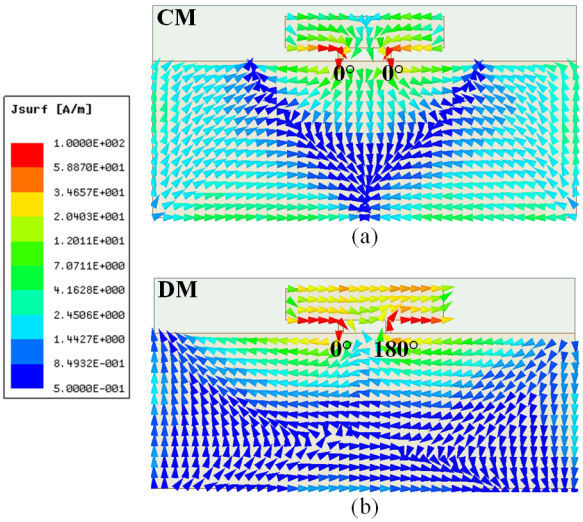

Fig. 3. Vector current distributions of the planar self-decoupled antenna pair with different feeding schemes. (a) CM feed. (b) DM feed.

The vector current distributions of the antenna pair with CM and DM feeding are shown in Fig. 3. When fed through CM signal, as shown in Fig. 3(a), the current is out of phase in the shared radiator with two folded monopole-like current distributions. When fed through DM signal, as shown in Fig. 3(b), the current is in phase in the shared radiator with a horizontal dipole-like current distribution. The active reflection coefficients of CM and DM are shown in Fig. 4. Due to the impact of the inverse ground mirror current for the horizontal dipole-like mode, the DM impedance is more dispersed than CM impedance with a longer curve in Smith chart as shown in Fig. 4. Nevertheless, we could also tune the CM and DM impedances to a similar status for achieving a good isolation. As seen, the feeding distance D_0 is a key parameter to tune the impedances of both CM and DM. The distance between CM and DM could be effectively altered by varying the feeding distance D_0, and an optimized self-isolation performance can be realized when $D_0 = 9$ mm. The simulated S-parameters in this case are shown in Fig. 5, the isolation between port1 and port2 is better than 11.5 dB across 3.3–4.2 GHz with a peak value of 23.2 dB at 3.65 GHz. The reflection coefficients of both port1 and port2 are less than −6 dB across the entire operating band.

Authorized licensed use limited to: Tsinghua University. Downloaded on July 21,2020 at 08:32:09 UTC from IEEE Xplore. Restrictions apply.

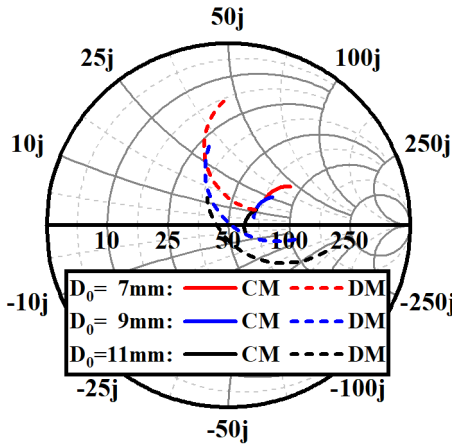

Fig. 4. Simulated Smith chart of CM and DM reflection coefficients with the feeding distance D_0 varied.

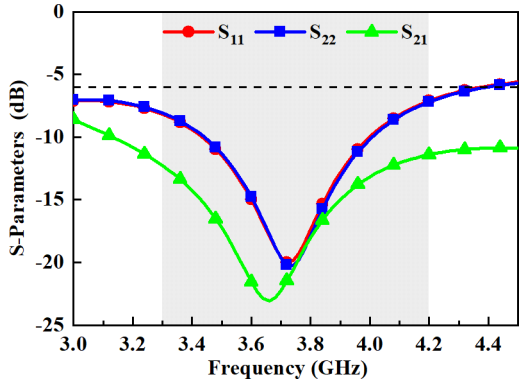

Fig. 5. Simulated S-parameters of the planar self-decoupled MIMO antenna pair.

To offer an intuitive insight of the decoupling performance, the current distributions of the proposed shared-radiator antenna pair fed through port1 is illustrated in Fig. 6(a). Note that the scale is the same with that in Fig. 3, which is not shown for brevity. As seen, only the left half of the shared radiator is excited when fed through port1, and it performs as an L-shaped folded monopole-like current mode. For comparison, the current distribution of two separated L-shaped folded monopoles without center-connecting line is presented in Fig. 6(b). As seen, strong coupling is occurred between two adjacent folded monopoles with a strong surface wave in the ground plane; and the isolation between them is only 6 dB. We could readily comprehend this phenomenon from the view of CM and DM impedances. When the center-connecting line is cut off, as shown in Fig. 6(d), the impedance of DM is significantly affected due to the current mode break for the dipole-like mode, which has a current maximum in the center plane as shown in Fig. 3(b); on the contrary, the CM impedance almost keeps unchanged because it has a center current null as shown in Fig. 3(a). Thus, the large discrepancy of CM and DM impedances leads to the poor isolation for the separated folded monopoles. Also, the center-connecting line could construct a balanced impedance response for CM and DM, which contributes to the high isolation of the proposed design.

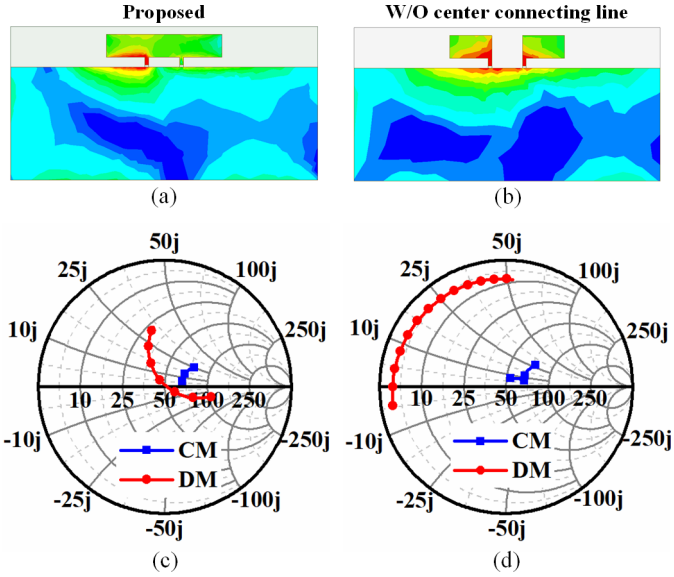

Fig. 6. Current distributions of the (a) proposed antenna pair and (b) separated folded monopoles when fed through port1. Smith chart of CM and DM reflection coefficients for the (c) proposed antenna pair and (d) separated folded monopoles.

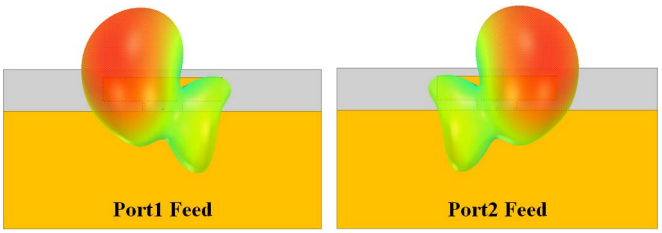

Fig. 7. 3-D radiation patterns of the planar self-decoupled MIMO antenna pair at 3.75 GHz when fed through (a) port1 and (b) port2.

C. Radiation and Diversity Performance

With the local current distribution in the shared radiator, a good radiation pattern diversity performance is achieved as shown in Fig. 7. When fed through port1, the radiation beam directs at the top left side with another half radiator served as a reflector. When fed through port2, on the contrary, the radiation beam directs at the top right side as shown in Fig. 7(b). The radiation pattern diversity performance can eliminate the spatial field coupling between two antenna elements.

To evaluate the diversity performance of the proposed MIMO antenna pair, the ECC is calculated by the simulated radiated far-field based on the formulation

$$\rho_e \approx |\rho_c|^2 = \left|\frac{\oint\!\!\oint A_{12}(\theta,\varphi)\sin\theta \mathrm{d}\theta\mathrm{d}\varphi}{\oint\!\!\oint A_{11}(\theta,\varphi)\sin\theta \mathrm{d}\theta\mathrm{d}\varphi \cdot \oint\!\!\oint A_{22}(\theta,\varphi)\sin\theta \mathrm{d}\theta\mathrm{d}\varphi}\right|^2 \tag{8}$$

where

$$A_{ij} = E_{\theta,i}(\theta,\varphi)\cdot E^*_{\theta,j}(\theta,\varphi) + E_{\varphi,i}(\theta,\varphi)\cdot E^*_{\varphi,j}(\theta,\varphi). \tag{9}$$

Here, $E_{\theta,i}$ and $E_{\varphi,i}$ are the complex electric field of port i in the elevation and azimuth planes, respectively, and $()*$ is the conjugate operator. As shown in Fig. 8, a good diversity

Authorized licensed use limited to: Tsinghua University. Downloaded on July 21,2020 at 08:32:09 UTC from IEEE Xplore. Restrictions apply.

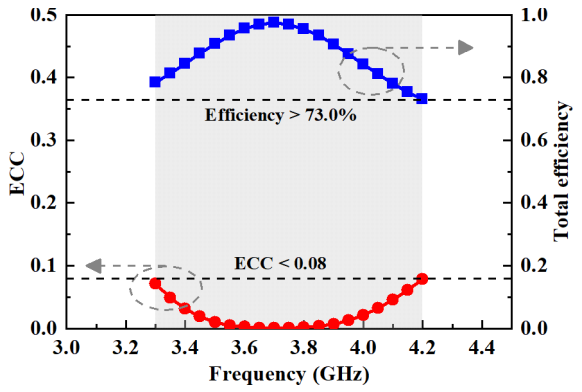

Fig. 8. Simulated ECC between port1 and port2 and total efficiency of the proposed planar self-decoupled MIMO antenna pair.

performance with the simulated ECC less than 0.08 across 3.3–4.2 GHz is obtained. The simulated total efficiency fed through port1 (or port2) is also reported in Fig. 8 to estimate the loss of the proposed MIMO system, and a high antenna efficiency of large than 73.0% is realized with an average value of 87.5% across the entire operating band.

IV. Design of the 8 × 8 MIMO Antenna System

A. Antenna Structure

The feasibility of the planar self-decoupling antenna pair has been effectively verified in Section III. Then, to reduce the ground clearance for the practical application, the shared radiator is folded into the side frame as shown in Fig. 9(a). By placing four sets of folded self-decoupled antenna pairs along the left and right side rims of the smartphone, an 8 × 8 MIMO system could be readily fulfilled as shown in Fig. 9(b).

A metal ground plane, with a dimension of 150 × 71 mm^2, is printed at the top side of the FR-4 ($\varepsilon_r = 4.4$, $\tan\delta = 0.02$) substrate (150 × 75 × 0.8 mm^3) to mimic the main board of the smartphone. The ground clearance is set to 2 mm at both sides for realizing an acceptable bandwidth. Two 0.8 mm-thick side FR-4 substrates are perpendicularly mounted at both sides of the main board to imitate the rims of the smartphone. The shared radiators are printed on the side FR-4 substrates and separated by a distance of 70 mm for a good isolation between antenna pairs.

Due to the impact of folding, the bandwidth response of the folded antenna pair is slightly different from the planar antenna pair. Hence the antenna size is reoptimized by HFSS, and the final detailed dimensions are L = 30 mm, H = 7.5 mm, D = 7.2 mm, G = 2 mm, and L_0 = 70 mm.

B. Parameter Analysis

To exhibit the design and optimized process, some key parameters are studied here to analyze their impact on the reflection coefficients and isolation of the antenna pair.

The height H is a vital parameter to affect the antenna bandwidth. As shown in Fig. 10(a) and (b), the isolated bandwidth could be enhanced with the increase in H while the matched bandwidth almost keeps unchanged. Thus, a wider overlapping

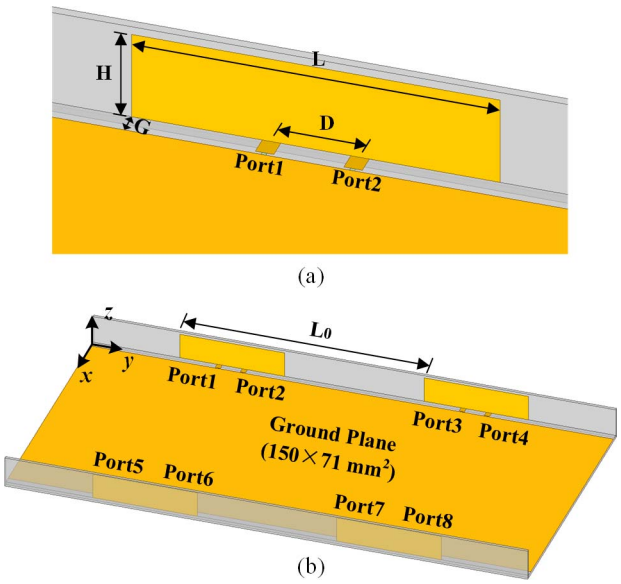

Fig. 9. (a) Geometry of the folded self-decoupled antenna pair. (b) Configuration of the 8 × 8 MIMO system based on the folded self-decoupled antenna pair. Detailed dimensions: L = 30 mm, H = 7.5 mm, D = 7.2 mm, G = 2 mm, and L_0 = 70 mm.

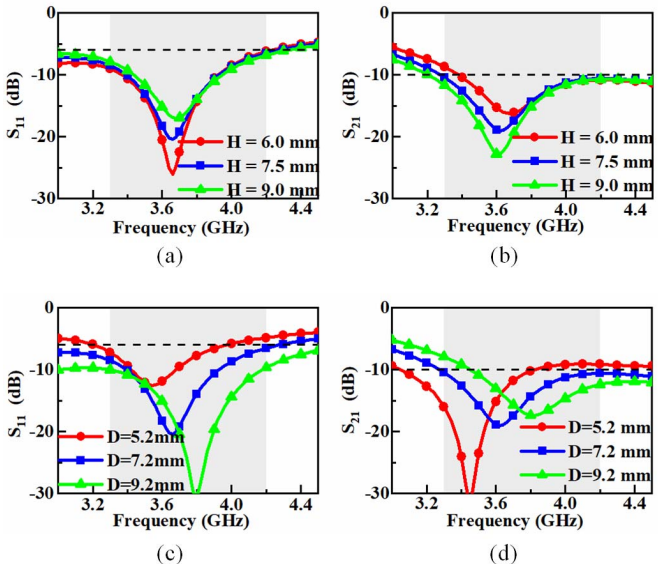

Fig. 10. Parameter analysis. (a) S_{11} and (b) S_{21} of the proposed antenna pair with different values of the height H. (c) S_{11} and (d) S_{21} of the proposed antenna pair with different values of the feeding distance D.

bandwidth could be realized with a higher height H, and H is set to 7.5 mm to accommodate the up-to-date smartphones.

As shown in Fig. 10(c) and (d), the impact of the feeding distance D is analyzed. With the increase in the feeding distance D, the S_{11} bandwidth is remarkably enhanced, but the isolated band is moved to the higher band. Therefore, the feeding distance D should be finely optimized to satisfy the bandwidth requirement of 3.3–4.2 GHz for both S_{11} and S_{21}.

C. Antenna Fabrication

As shown in Fig. 11, a prototype was fabricated to demonstrate the feasibility of the proposed 8 × 8 MIMO antenna system in experiment. The main board and two side boards

Authorized licensed use limited to: Tsinghua University. Downloaded on July 21,2020 at 08:32:09 UTC from IEEE Xplore. Restrictions apply.

TABLE I
COMPARISONS OF THE DECOUPLED ANTENNA PAIRS FOR 5G SMARTPHONES

Ref.	Decoupling Mechanism	Shared Radiator	Bandwidth	Size of Ant. Pair (L × H × W)	Isolation of Ant. Pair	Efficiency
[35]	Neutralization line	×	3.4-3.6 GHz (200 MHz)	[b]19×3 mm^2	>10 dB	40~60%
[36]	Asymmetrically mirrored	×	3.4-3.6 GHz (200 MHz)	10×7×1 mm^3	>10 dB	40-52%
[41]	Orthogonal mode	×	3.4-3.6 GHz (200 MHz)	12×7×1.8 mm^3	>20 dB	49~72.9%
[42]	Orthogonal mode	×	3.4-3.6 GHz (200 MHz)	28.3×5×3.6 mm^3	>21.8 dB	\
[43]	Orthogonal mode	√	3.4-3.6 GHz (200 MHz)	25×7×1.5 mm^3	>20.1 dB	35.2-64.7%
[38]	Grounded strip	×	3.4-3.6 GHz (200 MHz) 4.8-5.0 GHz (200 MHz)	22×7×1.8 mm^3	>17.5 dB >20 dB	>50%
[46]	Grounded strip	×	3.3-6.0 GHz (2700 MHz)	35×7×1 mm^3	>12 dB	56~83%
[47]	Grounded strip with capacitance	√	[a]3.3-4.0 GHz (700 MHz)	[c]20×6 mm^2	>12 dB	52~74%
Proposed	Self-decoupled	√	3.3-4.2 GHz (900 MHz)	30×7.5×2 mm^3	>10.5 dB	63.1~85.1%

[a] The measured reflection coefficients are less than -5 dB across the band.
[b] The building block is a planar structure with a length of 19 mm and ground clearance of 3 mm.
[c] The building block is planar structure with a length of 20 mm and ground clearance of 6 mm.

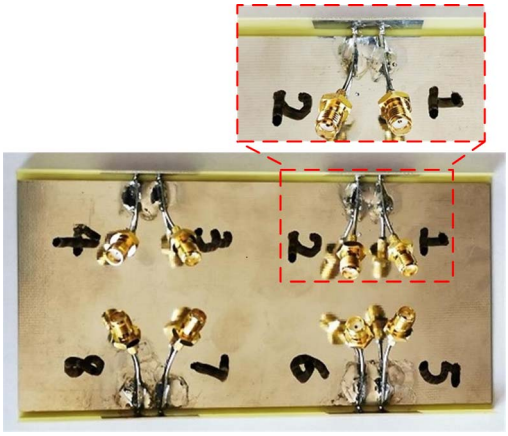

Fig. 11. Photograph of the proposed 5G 8 × 8 MIMO antenna system. Inset: the enlarged view of the self-decoupled antenna pair.

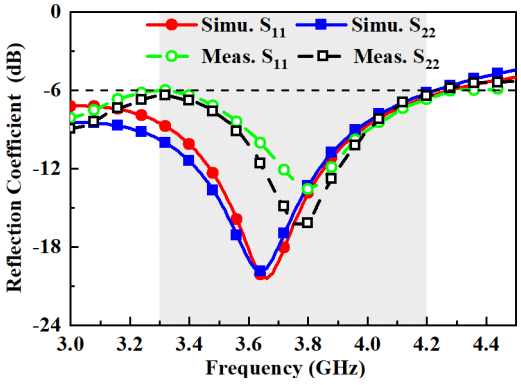

Fig. 12. Simulated and measured reflection coefficients of the proposed 8 × 8 MIMO system.

are manufactured by 0.8 mm-thick FR-4 substrates. The feed lines in the main board are soldered with the shared radiators in side boards for a good electric connection and fixture as shown in the inset. Eight 50 Ω semirigid cables are utilized to feed the eight ports for antenna test.

D. Simulated and Measured Results

The simulated and measured reflection coefficients of the proposed 8 × 8 MIMO system are reported in Fig. 12. Due to the structure symmetry, only the reflection coefficients of port1 and port2 are shown for brevity. Both the simulated and measured reflection coefficients are better than −6 dB across the desired N77 band from 3.3 to 4.2 GHz. Small frequency shift is occurred between the simulated and measured results owing to the manual fabrication error and the impact of the test semirigid cables.

The simulated and measured isolations and ECCs between every antenna pair are shown in Fig. 13. Note that the ECCs are calculated by the measured far-field based on (8) and (9).

For antenna pair1, the simulated and measured isolations between port1 and port2 are better than 10.5 dB and the measured ECC between them is less than 0.2, indicating a good self-decoupling and diversity performance for the antenna pair. For antenna pairs 1 and 2, both the simulated and measured isolations are better than 12.0 dB between every port, and the measured ECCs are less than 0.05.

For antenna pairs 1 and 3, with the help of the separation of the ground plane, a high isolation of better than 27.0 dB and a good diversity performance of ECCs < 0.007 are achieved across the desired band.

For antenna pairs 1 and 4, the isolations and ECCs between all ports are satisfactory due to the large distance.

Authorized licensed use limited to: Tsinghua University. Downloaded on July 21,2020 at 08:32:09 UTC from IEEE Xplore. Restrictions apply.

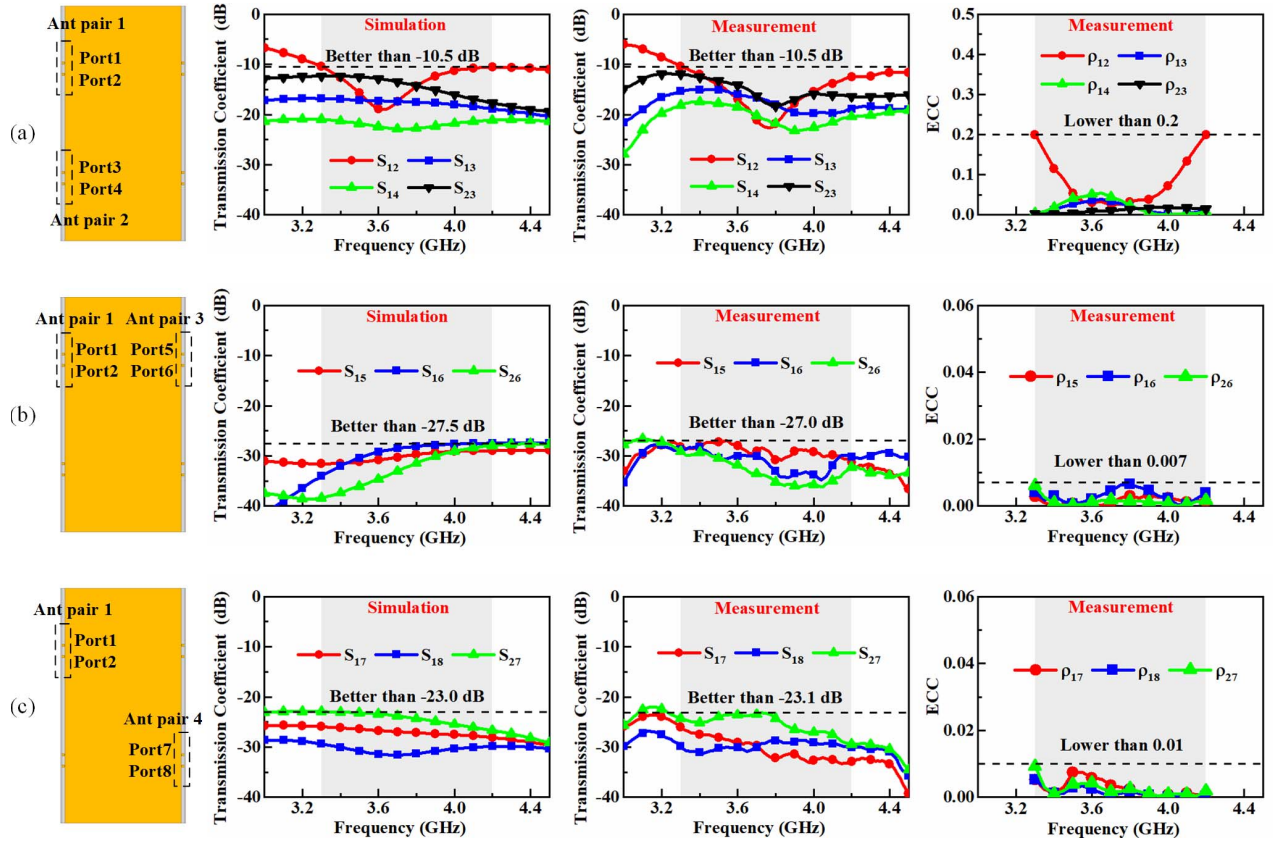

Fig. 13. Simulated and measured isolations and measured ECCs between (a) antenna pair 1 and antenna pair 2, (b) antenna pair 1 and antenna pair 3, and (c) antenna pair 1 and antenna pair 4.

The measured isolations are better than 23.1 dB and ECCs are lower than 0.01.

In a word, the isolations between all ports are better than 10.5 dB and ECCs between all ports are lower than 0.2 across 3.3–4.2 GHz for the proposed eight-element MIMO system, which can meet the standard of 5G smartphones.

The simulated and measured total efficiencies are shown in Fig. 14. As can be seen, the simulated total efficiency is 64.0%–90.9% with an average value of 79.1% for Ant1 and 62.8%–87.2% with an average value of 76.9% for Ant2. The measured efficiencies are in line with the simulated results. The measured efficiency is from 63.1% to 85.1% for both Ant1 and Ant2, with an average value of 76.5% for Ant1 and 75.9% for Ant2. The antenna efficiency is higher than the up-to-date 5G MIMO smartphone antenna with the help of the simple antenna structure, good impedance matching, and isolation.

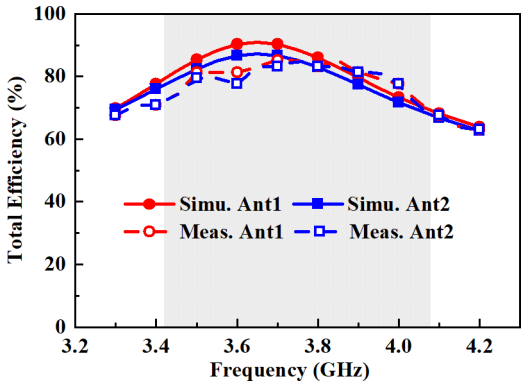

Fig. 14. Simulated and measured total efficiencies of the proposed 8 × 8 MIMO system.

E. Comparison

To highlight the merits of the proposed self-decoupled antenna pair, a comprehensive comparison table (Table I) is presented to compare this work with other decoupling techniques for closely spaced or shared-radiator antenna pairs. As seen, most of the decoupling techniques [35], [36], [38], [41]–[43] are narrow band and can only cover 3.4–3.6 GHz in the closely spaced configurations, which is not a good candidate for the global 5G NR service. Wong *et al.* [46] proposed a wideband (3.3–6.0 GHz) antenna pair decoupled by two symmetric grounded strip; however, the two elements are separated by a large distance of 19 mm (center by center) and possess complex structures. To enhance the integrated level of the structure in [46], the two elements are merged together as a shared radiator in [47], and a lumped capacitance is loaded in the center grounded strip to form an *LC* tank for current blocking; however, the bandwidth is significantly reduced from 2700 to 700 MHz with a large ground clearance of 6 mm. As a result, it is hard to implement wideband antenna pairs within a shared radiator by conventional decoupling techniques. In this article, a simple self-decoupling structure with both wideband and shared radiator is

Authorized licensed use limited to: Tsinghua University. Downloaded on July 21,2020 at 08:32:09 UTC from IEEE Xplore. Restrictions apply.

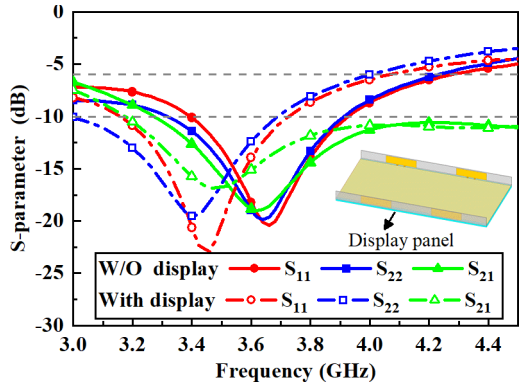

Fig. 15. Simulated S-parameters of the proposed 8 × 8 MIMO system with and without the display panel.

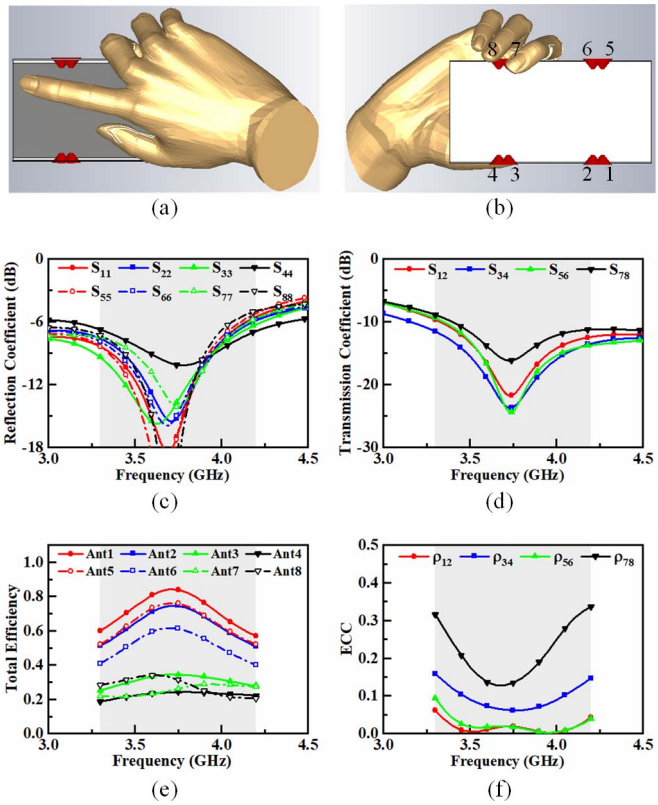

Fig. 16. Simulated antenna performance for the proposed 8 × 8 MIMO system with user's hand effects. (a) Front view of the single-handhold scenario. (b) Back view of the single-handhold scenario. (c) Reflection coefficient. (d) Transmission coefficient. (e) Total efficiency. (f) ECC.

achieved without using any extra decoupled structure, which is a promising candidate for the future highly integrated MIMO antennas for 5G applications. Moreover, an MCM, based on the cancellation of CM and DM, is presented for the first time, which could offer a systemic design guideline and create a new perspective for the antenna decoupling.

V. Practical Application Discussion

A. Display Panel Effects

To analyze the effects of the display panel in practical smartphone applications, the simulated S-parameters with and without the display panel are shown in Fig. 15. The display panel, with a dimension of 150 × 75 × 2 mm^3, is placed beneath the ground plane and made by the glass material ($\varepsilon_r = 5.5$). Owing to the influence of the high permittivity display panel, both of the reflection coefficient and isolation are shifted to the lower band, but the impedance matching and isolation performance are not broken. Thus, the operating frequency can be easily tuned to the desired band by scaling down the antenna size.

B. User's Hand Effects

The user's hand, which has a high permittivity and high loss characteristic in the microwave spectrum, shows great influence on the antenna performance. To analyze the effects of the user's hand, the 8 × 8 MIMO antenna system under the single-handhold scenario is modeled and simulated in CST Microwave Studio. The front and back views of the simulation model are shown in Fig. 16(a) and (b), respectively. Also, the simulated results with user's hand effects are proposed in Fig. 16(c)–(f). As seen, the reflection coefficient and isolation almost keep unchanged for all antenna elements. However, the total efficiencies of Ant3, Ant4, Ant7 and Ant8 are significantly deteriorated owing to the absorbing effect of user's hand. Meanwhile, the ECC between Ant7 and Ant8 is also affected with the impact of user's fingers.

VI. Conclusion

In this article, a simple wideband self-decoupled MIMO antenna pair with a shared radiator is proposed. Also, an MCM is developed to provide a systemic design guideline for the proposed self-decoupling scheme. In the MCM, the current mode fed through port1 (or port2) could be equivalent to the superposition of CM and DM, and a good self-isolation performance could be realized by tuning the CM and DM active impedances as similar as possible. By utilizing this strategy, a planar self-decoupled MIMO antenna pair with a shared radiator is realized. It could offer a wide bandwidth of 3.3–4.2 GHz with both $S_{11} < -6$ dB and $S_{21} < -11.5$ dB. Moreover, a high antenna efficiency of 73%–97% and a good diversity performance of ECC < 0.08 are also achieved. Then, the concept of self-decoupled antenna pair is applied to the 8 × 8 MIMO system for 5G smartphone applications. The measured results demonstrate that the 8 × 8 MIMO system has a good isolation of better than 10.5 dB between all eight ports and possesses a high efficiency of 63.1%–85.1% across the 5G N77 band (3.3–4.2 GHz).

The proposed design scheme impels the MIMO antenna to a higher integration level by the novel self-decoupling strategy. We forecast that the proposed design scheme, with the merits of self-decoupling, shared radiator, simple structure, wide bandwidth, and high efficiency, has the potential for the future highly integrated MIMO antenna, especially for the 5G smartphone applications.

References

[1] J. G. Andrews *et al.*, "What will 5G be?" *IEEE J. Sel. Areas Commun.*, vol. 32, no. 6, pp. 1065–1082, Jun. 2014.

Authorized licensed use limited to: Tsinghua University. Downloaded on July 21,2020 at 08:32:09 UTC from IEEE Xplore. Restrictions apply.

[2] E. Biglieri, *MIMO Wireless Communications*. Cambridge, U.K.: Cambridge Univ. Press, 2010.

[3] Z. Zhang, *Antenna Design for Mobile Devices*, 2nd ed. Hoboken, NJ, USA: Wiley, 2017.

[4] X. Chen, S. Zhang, and Q. Li, "A review of mutual coupling in MIMO systems," *IEEE Access*, vol. 6, pp. 24706–24719, 2018.

[5] F. Yang and Y. Rahmat-Samii, "Microstrip antennas integrated with electromagnetic band-gap (EBG) structures: A low mutual coupling design for array applications," *IEEE Trans. Antennas Propag.*, vol. 51, no. 10, pp. 2936–2946, Oct. 2003.

[6] A. Diallo, C. Luxey, P. Le Thuc, R. Staraj, and G. Kossiavas, "Study and reduction of the mutual coupling between two mobile phone PIFAs operating in the DCS1800 and UMTS bands," *IEEE Trans. Antennas Propag.*, vol. 54, no. 11, pp. 3063–3074, Nov. 2006.

[7] Y. Wang and Z. Du, "A wideband printed dual–antenna system with a novel neutralization line for mobile terminals," *IEEE Antennas Wireless Propag. Lett.*, vol. 12, pp. 1428–1431, Oct. 2013.

[8] Y. Wang and Z. Du, "A wideband printed dual–antenna with three neutralization lines for mobile terminals," *IEEE Trans. Antennas Propag.*, vol. 62, no. 3, pp. 1495–1500, Mar. 2014.

[9] A. Mak, C. Rowell, and R. Murch, "Isolation enhancement between two closely packed antennas," *IEEE Trans. Antennas Propag.*, vol. 56, no. 11, pp. 3411–3419, Nov. 2008.

[10] B. K. Lau and J. B. Andersen, "Simple and efficient decoupling of compact arrays with parasitic scatterers," *IEEE Trans. Antennas Propag.*, vol. 60, no. 2, pp. 464–472, Feb. 2012.

[11] S. Chang, Y.-S. Wang, and S.-J. Chung, "A decoupling technique for increasing the port isolation between strongly coupled antennas," *IEEE Trans. Antennas Propag.*, vol. 56, no. 12, pp. 3650–3658, Dec. 2008.

[12] S. Zhang, B. K. Lau, Y. Tan, Z. Ying, and S. He, "Mutual coupling reduction of two PIFAs with a T–shape slot impedance transformer for MIMO mobile terminals," *IEEE Trans. Antennas Propag.*, vol. 60, no. 3, pp. 1521–1531, Mar. 2012.

[13] S. Hong, K. Chung, J. Lee, S. Jung, S.-S. Lee, and J. Choi, "Design of a diversity antenna with stubs for UWB applications," *Microw. Opt. Technol. Lett.*, vol. 50, no. 5, pp. 1352–1356, May 2008.

[14] J. Sui and K.-L. Wu, "Self–curing decoupling technique for two inverted–F antennas with capacitive loads," *IEEE Trans. Antennas Propag.*, vol. 66, no. 3, pp. 1093–1101, Mar. 2018.

[15] K.-L. Wu, C. Wei, X. Mei, and Z.-Y. Zhang, "Array–antenna decoupling surface," *IEEE Trans. Antennas Propag.*, vol. 65, no. 12, pp. 6728–6738, Dec. 2017.

[16] K. Wei, Z. Zhang, W. Chen, and Z. Feng, "A novel hybrid–fed patch antenna with pattern diversity," *IEEE Antennas Wireless Propag. Lett.*, vol. 9, pp. 562–565, 2010.

[17] Y. Li, Z. Zhang, W. Chen, Z. Feng, and M. F. Iskander, "A dual-polarization slot antenna using a compact CPW feeding structure," *IEEE Antennas Wireless Propag. Lett.*, vol. 9, pp. 191–194, 2010.

[18] C. Deng, Y. Li, Z. Zhang, and Z. Feng, "A wideband high-isolated dual-polarized patch antenna using two different balun feedings," *IEEE Antennas Wireless Propag. Lett.*, vol. 13, pp. 1617–1619, 2014.

[19] C. Deng, X. Lv, and Z. Feng, "Wideband dual-mode patch antenna with compact CPW feeding network for pattern diversity application," *IEEE Trans. Antennas Propag.*, vol. 66, no. 5, pp. 2628–2633, May 2018.

[20] L. Sun, Y. Li, Z. Zhang, and M. F. Iskander, "A compact planar omnidirectional MIMO array antenna with pattern phase diversity using folded dipole element," *IEEE Trans. Antennas Propag.*, vol. 67, no. 3, pp. 1688–1696, Mar. 2019.

[21] J.-Y. Deng, J. Yao, D.-Q. Sun, and L.-X. Guo, "Ten-element MIMO antenna for 5G terminals," *Microw. Opt. Technol. Lett.*, vol. 60, no. 12, pp. 3045–3049, Dec. 2018.

[22] J. Guo, L. Cui, C. Li, and B. Sun, "Side-edge frame printed eight-port dual-band antenna array for 5G smartphone applications," *IEEE Trans. Antennas Propag.*, vol. 66, no. 12, pp. 7412–7417, Dec. 2018.

[23] D. Huang, Z. Du, and Y. Wang, "Slot antenna array for 5G metal frame mobile phone applications," *Int. J. RF Microw. Comput. Aided Eng.*, vol. 29, Sep. 2019, Art. no. e21841.

[24] D. Q. Liu, M. Zhang, H. J. Luo, H. L. Wen, and J. Wang, "Dual-band platform-free PIFA for 5G MIMO application of mobile devices," *IEEE Trans. Antennas Propag.*, vol. 66, no. 11, pp. 6328–6333, Nov. 2018.

[25] X. Zhang, Y. Li, W. Wang, and W. Shen, "Ultra–wideband 8-port MIMO antenna array for 5G metal–frame smartphones," *IEEE Access*, vol. 7, pp. 72273–72282, 2019.

[26] A. Zhao and Z. Ren, "Wideband MIMO antenna systems based on coupled–loop antenna for 5G–N77/N78/N79 applications in mobile terminals," *IEEE Access*, vol. 7, pp. 93761–93771, 2019.

[27] X. Zhao, S. P. Yeo, and L. C. Ong, "Decoupling of inverted–F antennas with high–order modes of ground plane for 5G mobile MIMO platform," *IEEE Trans. Antennas Propag.*, vol. 66, no. 9, pp. 4485–4495, Sep. 2018.

[28] M.-Y. Li *et al.*, "Eight–port orthogonally dual–polarized antenna array for 5G smartphone applications," *IEEE Trans. Antennas Propag.*, vol. 64, no. 9, pp. 3820–3830, Sep. 2016.

[29] W. Jiang, B. Liu, Y. Cui, and W. Hu, "High–isolation eight–element MIMO array for 5G smartphone applications," *IEEE Access*, vol. 7, pp. 34104–34112, 2019.

[30] H. Xu, H. Zhou, S. Gao, H. Wang, and Y. Cheng, "Multimode decoupling technique with independent tuning characteristic for mobile terminals," *IEEE Trans. Antennas Propag.*, vol. 65, no. 12, pp. 6739–6751, Dec. 2017.

[31] A. Zhao and Z. Ren, "Size reduction of self-isolated antenna MIMO antenna system for 5G mobile phone applications," *IEEE Antennas Wireless Propag. Lett.*, vol. 18, no. 1, pp. 152–156, Jan. 2019.

[32] Y. Li, C.-Y.-D. Sim, Y. Luo, and G. Yang, "High-isolation 3.5-GHz 8-antenna MIMO array using balanced open slot antenna element for 5G smartphones," *IEEE Trans. Antennas Propag.*, vol. 67, no. 6, pp. 3820–3830, Jun. 2019.

[33] M.-Y. Li, Z.-Q. Xu, Y.-L. Ban, C.-Y.-D. Sim, and Z.-F. Yu, "Eight-port orthogonally dual-polarized MIMO antennas using loop structures for 5G smartphone," *IET Microw., Antennas Propag.*, vol. 11, no. 12, pp. 1810–1816, Nov. 2017.

[34] M.-Y. Li, Y.-L. Ban, Z.-Q. Xu, J. Guo, and Z.-F. Yu, "Tri-polarized 12-antenna MIMO array for future 5G smartphone applications," *IEEE Access*, vol. 6, pp. 6160–6170, 2017.

[35] K.-L. Wong, J.-Y. Lu, L.-Y. Chen, W.-Y. Li, and Y.-L. Ban, "8-antenna and 16-antenna arrays using the quad-antenna linear array as a building block for the 3.5-GHz LTE MIMO operation in the smartphone," *Microw. Opt. Technol. Lett.*, vol. 58, no. 1, pp. 174–181, Jan. 2016.

[36] K.-L. Wong, C.-Y. Tsai, and J.-Y. Lu, "Two asymmetrically mirrored gap-coupled loop antennas as a compact building block for eight antenna MIMO array in the future smartphone," *IEEE Trans. Antennas Propag.*, vol. 65, no. 4, pp. 1765–1778, Apr. 2017.

[37] Z. Ren, A. Zhao, and S. Wu, "MIMO antenna with compact decoupled antenna pairs for 5G mobile terminals," *IEEE Antennas Wireless Propag. Lett.*, vol. 18, no. 7, pp. 1367–1371, Jul. 2019.

[38] Z. Ren and A. Zhao, "Dual-band MIMO antenna with compact self-decoupled antenna pairs for 5G mobile applications," *IEEE Access*, vol. 7, pp. 82288–82296, 2019.

[39] C. Deng, D. Liu, and X. Lv, "Tightly arranged four-element MIMO antennas for 5G mobile terminals," *IEEE Trans. Antennas Propag.*, vol. 67, no. 10, pp. 6353–6361, Oct. 2019.

[40] L. Sun, H. Feng, Y. Li, and Z. Zhang, "Tightly arranged orthogonal mode antenna for 5G MIMO mobile terminals," *Microw. Opt. Technol. Lett.*, vol. 60, no. 7, pp. 1751–1756, Jul. 2018.

[41] L. Sun, H. Feng, Y. Li, and Z. Zhang, "Compact 5G MIMO mobile phone antennas with tightly arranged orthogonal-mode pairs," *IEEE Trans. Antennas Propag.*, vol. 66, no. 11, pp. 6364–6369, Nov. 2018.

[42] H. Xu, S. Gao, H. Zhou, H. Wang, and Y. Cheng, "A highly integrated MIMO antenna unit: Differential/common mode design," *IEEE Trans. Antennas Propag.*, vol. 67, no. 11, pp. 6724–6734, Nov. 2019.

[43] L. Chang, Y. Yu, K. Wei, and H. Wang, "Polarization-orthogonal co-frequency dual-antenna pair suitable for 5G MIMO smartphone with metallic bezels," *IEEE Trans. Antennas Propag.*, vol. 67, no. 8, pp. 5212–5220, Aug. 2019.

[44] A. Ren, Y. Liu, and C.-Y.-D. Sim, "A compact building block with two shared-aperture antennas for eight-antenna MIMO array in metal-rimmed smartphone," *IEEE Trans. Antennas Propag.*, vol. 67, no. 10, pp. 6430–6438, Oct. 2019.

[45] *5G NR (New Radio)*. Accessed: May 28, 2019. [Online]. Available: http://3gpp.org/

[46] K.-L. Wong, Y.-H. Chen, and W.-Y. Li, "Decoupled compact ultra-wideband MIMO antennas covering 3300–6000 MHz for the fifth-generation mobile and 5GHz-WLAN operations in the future smartphone," *Microw. Opt. Technol. Lett.*, vol. 60, no. 10, pp. 2345–2351, Oct. 2018.

[47] K.-L. Wong, B.-W. Lin, and S.-E. Lin, "High-isolation conjoined loop multi-input multi-output antennas for the fifth-generation tablet device," *Microw. Opt. Technol. Lett.*, vol. 61, no. 1, pp. 111–119, Jan. 2019.

[48] D. M. Pozar, *Microwave Engineering*, 2nd ed. New York, NY, USA: Wiley, 1998.

Authorized licensed use limited to: Tsinghua University. Downloaded on July 21,2020 at 08:32:09 UTC from IEEE Xplore. Restrictions apply.

Libin Sun (Student Member, IEEE) received the B.S. degree from Xidian University, Xi'an, China, in 2016. He is currently pursuing the Ph.D. degree with the Department of Electrical and Engineering, Tsinghua University, Beijing, China.

His current research interests include antenna design and theory, particularly in 5G terminal antennas, MIMO and diversity antennas, circularly polarized antennas, leaky-wave antennas, and surface-wave antennas.

Mr. Sun was a recipient of the Top 50 Outstanding Reviewer Award for the IEEE TRANSACTIONS ON ANTENNAS AND PROPAGATION in 2019 and the Chinese National Scholarship in 2014, 2015, and 2019. He serves as a Reviewer for the IEEE TRANSACTIONS ON ANTENNAS AND PROPAGATION, IEEE ANTENNAS AND WIRELESS PROPAGATION LETTERS, the IEEE ACCESS, *IET Electronics Letters*, *Microwave and Optical Letters*, and *Computer Applications in Engineering Education*.

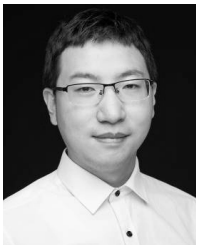

Yue Li (Senior Member, IEEE) received the B.S. degree in telecommunication engineering from Zhejiang University, Hangzhou, China, in 2007 and the Ph.D. degree in electronic engineering from Tsinghua University, Beijing, China, in 2012.

In June 2012, he joined the Department of Electronic Engineering, Tsinghua University, as a Post-Doctoral Fellow. In December 2013, he joined the Department of Electrical and Systems Engineering, University of Pennsylvania, Philadelphia, PA, USA, as a Research Scholar. He was a Visiting Scholar with the Institute for Infocomm Research (I2R), A∗STAR, Singapore, in 2010 and also with the Hawaii Center of Advanced Communication (HCAC), University of Hawaii at Manoa, Honolulu, HI, USA, in 2012. Since January 2016, he has been with Tsinghua University, where he is currently an Assistant Professor and also an Associate Professor with the Department of Electronic Engineering. He has authored or co-authored over 90 journal articles and 45 international conference articles, and holds 15 granted Chinese patents. His current research interests include metamaterials, plasmonics, electromagnetics, nanocircuits, mobile and handset antennas, MIMO and diversity antennas, and millimeter-wave antennas and arrays.

Dr. Li was a recipient of the Issac Koga Gold Medal from URSI General Assembly in 2017, the Second Prize of Science and Technology Award of the China Institute of Communications in 2017, the Young Scientist Awards from the conferences of ACES 2018, AT-RASC 2018, AP-RASC 2016, EMTS 2016, and URSI GASS 2014, the best paper awards from the conferences of CSQRWC 2018, NCMMW 2018 and 2017, APCAP 2017, NCANT 2017, ISAPE 2016, and ICMMT 2016, the Outstanding Doctoral Dissertation of Beijing Municipality in 2013, and the Principal Scholarship of Tsinghua University in 2011. He is serving as an Associate Editor for the IEEE TRANSACTIONS ON ANTENNAS AND PROPAGATION, IEEE ANTENNAS AND WIRELESS PROPAGATION LETTERS, and *Computer Applications in Engineering Education*, and also serving on the Editorial Board of Scientific Report.

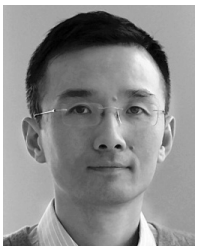

Zhijun Zhang (Fellow, IEEE) received the B.S. and M.S. degrees from the University of Electronic Science and Technology of China, Chengdu, China, in 1992 and 1995, respectively, and the Ph.D. degree from Tsinghua University, Beijing, China, in 1999.

In 1999, he joined the Department of Electrical Engineering, The University of Utah, Salt Lake City, UT, USA, as a Post-Doctoral Fellow, where he was appointed as Research Assistant Professor in 2001. In May 2002, he joined the University of Hawaii at Manoa, Honolulu, HI, USA, as an Assistant Researcher. In November 2002, he joined Amphenol T&M Antennas, Vernon Hills, IL, USA, as a Senior Staff Antenna Development Engineer and was then promoted to the position of Antenna Engineer Manager. In 2004, he joined Nokia Inc., San Diego, CA, USA, as a Senior Antenna Design Engineer. In 2006, he joined Apple Inc., Cupertino, CA, as a Senior Antenna Design Engineer and was then promoted to the position of Principal Antenna Engineer. Since August 2007, he has been with Tsinghua University, where he is currently a Professor with the Department of Electronic Engineering. He has authored *Antenna Design for Mobile Devices* (Wiley, 1st ed. 2011 and 2nd ed. 2017). He served as an Associate Editor for the IEEE TRANSACTIONS ON ANTENNAS AND PROPAGATION from 2010 to 2014 and IEEE ANTENNAS AND WIRELESS PROPAGATION LETTERS from 2009 to 2015.

Hanyang Wang (Senior Member, IEEE) received the Ph.D. degree from Heriot-Watt University, Edinburgh, U.K., in 1995.

From 1986 to 1991, he served as a Lecturer and an Associate Professor with Shandong University, Jinan, China. From 1995 to 1999, he was a Post-Doctoral Research Fellow with the University of Birmingham, Birmingham, U.K., and also with the University of Essex, Colchester, U.K. From 1999 to 2000, he was a Software Development and Microwave and Antenna Engineering Consultant Engineer with Vector Fields Ltd., Oxford, U.K. He joined Nokia U.K. Ltd., Farnborough, U.K., in 2001, where he was a Mobile Antenna Specialist for 11 years. After leaving Nokia, he joined Huawei Technology Ltd., Reading, U.K, where he is currently the Chief Mobile Antenna Expert and the Head of the Mobile Antenna Technology Division. He is also an Adjunct Professor with Nanjing University, Nanjing, China, and also with Sichuan University, Chengdu, China. His current research interests include small, wideband, and multiband antennas for mobile terminals, antennas, and antenna arrays for 5G mobile communications in sub-6 GHz and mm-Wave frequency bands. He has authored over 100 articles on these topics and holds over 40 granted U.S./European (EU)/Japan (JP)/Chinese (CN) patents.

Dr. Wang is a Huawei Fellow and an IET Fellow. He was a recipient of the Title of Nokia Inventor of the Year in 2005, the Nokia Excellence Award in 2011, the Huawei Individual Gold Medal Award in 2012, and the Huawei Team Gold Medal Award in 2013 and 2014. His patent was ranked number one among 2015 Huawei top ten patent awards. He is an Associate Editor of IEEE ANTENNAS AND WIRELESS PROPAGATION LETTERS.

Authorized licensed use limited to: Tsinghua University. Downloaded on July 21,2020 at 08:32:09 UTC from IEEE Xplore. Restrictions apply.